12. H.M. Hsiao, J.H. Lu, and J.W. Wu, Novel dual-broadband design of semicircular slot antenna for wireless communication, Microwave Opt Technol Lett 49 (2007), 2165–2169.
13. J. Tao, C.H. Cheng, and H.B. Zhu, Compact dual-band slot-antenna for WLAN applications, Microwave Opt Technol Lett 49 (2007), 1203–1204.

DEVELOPMENT OF DUAL-BAND MICROSTRIP PATCH ANTENNA FOR WLAN/MIMO/WiMAX/AMSAT/WAVE APPLICATIONS

Jaswinder Kaur and Rajesh Khanna
Department of Electronics and Communication Engineering, Thapar University, Patiala, 147004, Punjab, India; Corresponding author: jaswinder.kaur@thapar.edu

Received 30 July 2013

ABSTRACT: *The present work represents a dual-band microstrip-fed patch antenna in which the radiating structure is formed with a pair of inverted L-shaped patches and ground plane is being modified to a ┼ shape. Both the radiating patch and modified ground plane are perfect electric conductors. The patch is printed on a readily available Epoxy Glass (FR-4) substrate with thickness 1.6 mm, relative permittivity 4.4, and loss tangent 0.0024. The proposed microstrip patch antenna (MPA) design is capable of generating two distinct operating bands with 10-dB return loss as follows 3.34–3.54 GHz and 4.90–6.26 GHz with adequate bandwidth of 200 MHz and 1.36 GHz, respectively. The impedance bandwidths are wide enough to cover the required bandwidths of 3.3–3.5 GHz, 5.15–5.35 GHz, 5.725–5.825 GHz for wireless local area network, 3.3–3.5 GHz for multiple input multiple output, 5.25–5.85 GHz for world-wide interoperability for microwave access, 5.650–5.670 GHz for uplinks and 5.830–5.850 GHz for downlinks of Amateur Satellite, and 5.9 GHz wireless access in the vehicular environment (WAVE-IEEE 802.11p). Proposed MPA was simulated using Computer Simulation Technology Microwave Studio V9 based on the finite integration technique with perfect boundary approximation and effect of using different substrate materials was studied. Finally, the proposed antenna with optimized parameters was fabricated and some performance measurements were taken to validate against simulation results. The design procedure to achieve the required performance are presented and discussed.* © 2014 Wiley Periodicals, Inc. Microwave Opt Technol Lett 56:988–993, 2014; View this article online at wileyonlinelibrary.com. DOI 10.1002/mop.28206

Key words: *microstrip patch antenna; defected ground structure; dual-band; inverted L-shaped patches; WLAN/MIMO/WiMAX/AMSAT/WAVE; CST MWS V9*

1. INTRODUCTION

The design of a microstrip patch antenna (MPA) is one of the most exciting developments in electromagnetic history because

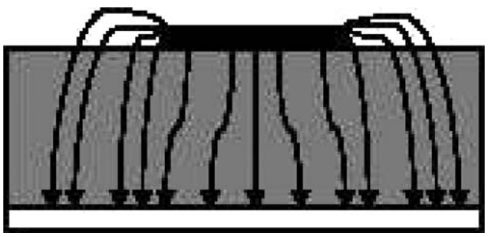

Figure 1 Electric field lines

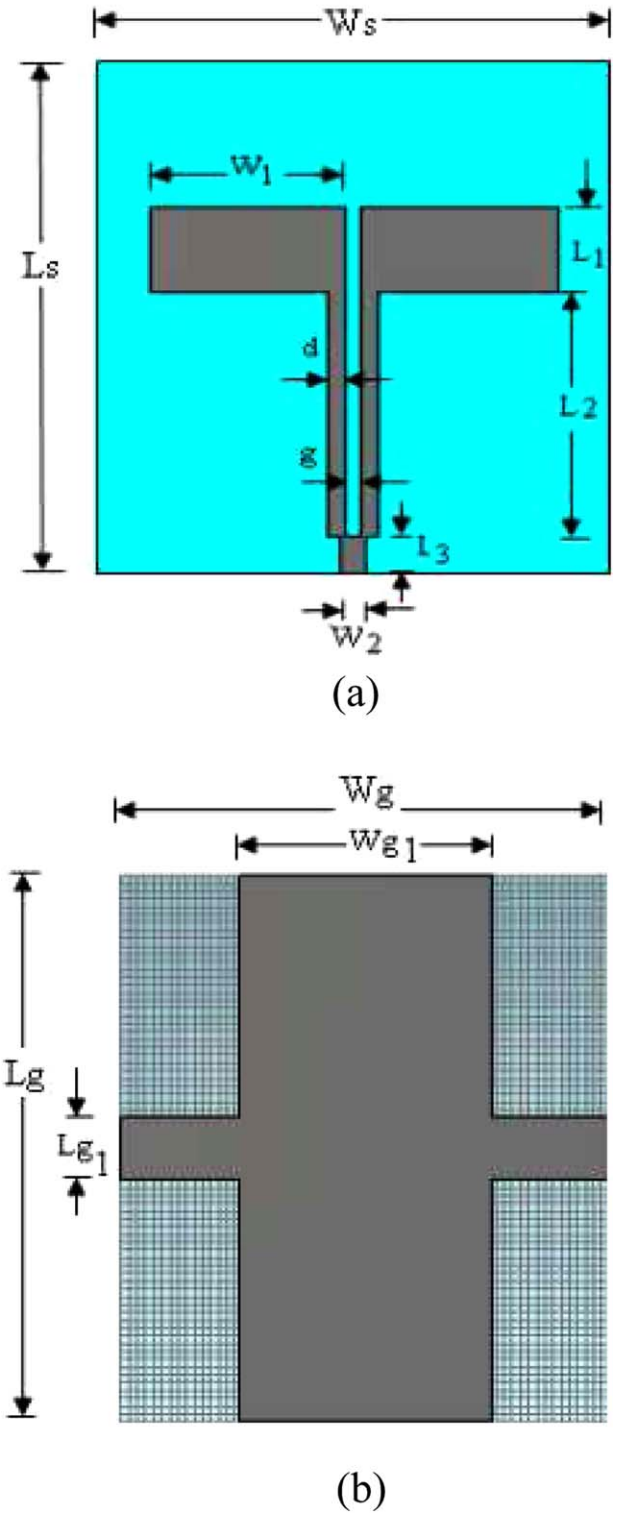

Figure 2 Antenna configuration of the proposed antenna front view, radiating structure and (b) back view, ┼-shaped ground plane. [Color figure can be viewed in the online issue, which is available at wileyonlinelibrary.com]

of its salient features which are not commonly exhibited in other antenna configurations including ease of fabrication, good radiation control, low cost of production, low profile, lightweight, simple, and inexpensive to fabricate using modern day printed circuit board technology, compatible with microwave and millimeter-wave integrated circuits, and ability to conform to

TABLE 1 Optimal Parameters of the Proposed MPA

Parameters	W_s	L_s	L_1	L_2	L_3	W_1	W_2	L_{g1}	W_{g1}	g	d
Unit (mm)	60	70	11.7	33.5	5	23	3	8	31	2	2

planar and non planar surfaces. These features are largely responsible for the success of MPA as a viable topic for new research. The performance and operation of a MPA is driven mainly by the geometry of the printed patch and the material characteristics of the substrate onto which the antenna is printed. Recently, the ability to integrate more than one communication standard into a single system has become an increasing demand of a modern portable wireless communication device. Also, a modern antenna requires not only the function of providing a dual or multiband operation but also a simple structure, compact size, high gain, and easy integration with the system circuit. Dual-band multifrequency systems combining various IEEE 802.11a/b/g standards are becoming more attractive [1]. A dual-band/wideband antenna is a key component for such communication systems [1–12]. Such dual-band antennas with single feed have been proposed in various configurations [1, 3–5, 7, 8]. These antennas either provide inadequate coverage at the specific resonating frequencies or they cannot be easily integrated in portable devices [1, 8]. Furthermore, the gains of reported single-fed dual-band antennas are lower than 6 dBi [1–9] and they face difficulty to meet the requirement for applications such as long-range communications or point-to-point communications devices running on battery. The main of the present work was to achieve high gain of wireless local area network (WLAN) antenna. Also, the size of antennas proposed in [10–14] is very large and complex which reduces an antenna's application in wireless communication.

In this article, a high-gain dual-band MPA having multifrequency operation formed with a pair of inverted L-shaped patches printed on a FR-4 substrate with defected ground structure (DGS) is presented for satisfying different wireless communication standards simultaneously. The constructed antenna has two inverted L-shaped patches separated by a small gap "g". These design skills are introduced to approach the excitation of dual-resonant modes because of two current paths accompanied with stable radiation characteristics over the entire operating band. The performance of the proposed antenna is simulated using commercial software Computer Simulation Technology Microwave Studio (CST MWS) V9, and the prototype of the antenna is manufactured and measured. From the measured results, the proposed antenna shows two operating frequency bands with 10-dB return loss as follows 3.34–3.54 and 4.90–6.26 GHz with adequate bandwidth of 200 MHz and 1.36 GHz, respectively. The obtained bandwidth of 1.36 GHz (4.90–6.26 GHz) for the upper resonating band is quite higher than the existing dual/multiband antenna designs and all this is because of the defected structure embedded in the ground plane which makes it suitable to be used in various wireless communication systems, namely, WLAN/world-wide interoperability for microwave access (WiMAX)/Amateur Satellite (AMSAT)/wireless access in the vehicular environment (WAVE). Both the inverted L-shaped patches and ┼-shaped ground plane play a very vital role to reject the interferences in desired frequency bands. The proposed antenna design has been studied thoroughly and fabricated, and the details of simulated and measured results are presented and discussed.

2. ANTENNA DESIGN

MPA consists of a radiating patch on one side of a dielectric substrate which has a ground plane on the other side as shown in Figure 2. Dielectric constant of the substrate (Єr) is typically in the range $2.2 < Єr < 12$ [15]. The radiating patch and the feed lines are usually photoetched on the dielectric substrate. MPAs radiate primarily because of the fringing fields between the patch edge and the ground plane as shown in Figure 1 [16, 17].

Figure 2 shows the geometry of the proposed antenna capable for dual-band operational characteristics. In our present design structure, the antenna is etched on both sides of FR-4 substrate with relative dielectric constant 4.4, thickness 1.6 mm, loss tangent 0.0024, and a total area $L_s \times W_s = 70 \times 60$ mm^2. Also, the substrate used is having the metal thickness of 0.07 mm. The radiating structure consists of a two inverted L-shaped patches located symmetrically along the center line and separated by a small gap "g" [Fig. 2(a)]. The dimensions of wide vertical and horizontal arms of L-shaped patches are denoted as L_1 and W_1. The symbol L_2 represents the length of narrow arm of L-shaped patches and "d" represents the width of narrow strips. Notice that, there is a symmetrical DGS having wide vertical arm with dimensions $L_g \times W_{g1} = 70 \times 31$ mm^2 and narrow horizontal arm with dimensions $W_g \times L_{g1} = 60 \times 8$ mm^2 printed on the back of the substrate. This ┼-shaped ground plane [Fig. 2(b)] is responsible for bandwidth enhancement of

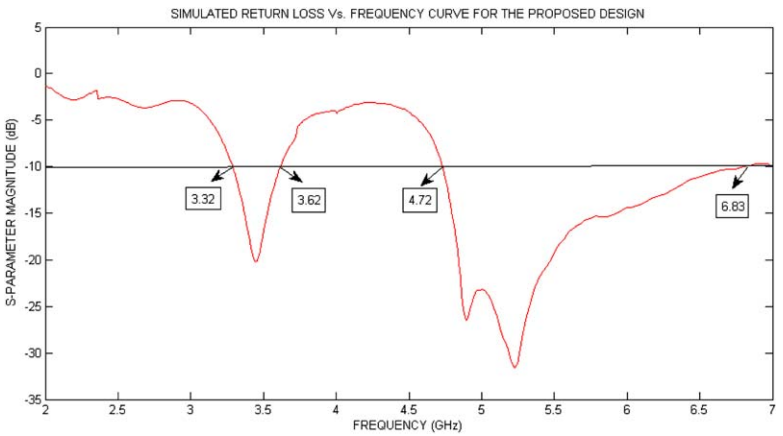

Figure 3 Simulated return loss curve of proposed antenna. [Color figure can be viewed in the online issue, which is available at wileyonlinelibrary.com]

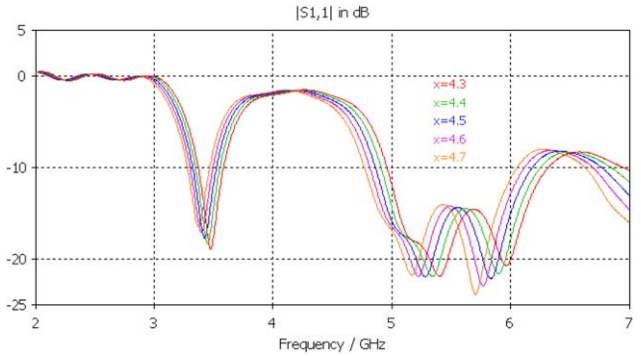

Figure 4 Optimization of dielectric constant of the substrate. [Color figure can be viewed in the online issue, which is available at wileyonlinelibrary.com]

the upper resonating band. For good radiation characteristics, the positions, lengths, and widths of a pair of inverted L-shaped patches and DGS were adjusted carefully. The gap "*g*" between two inverted L-shaped patches also plays a major role in the successful excitation of two appropriate desired resonating frequency bands.

The front and back view of proposed antenna has been shown in Figures 2(a) and 2(b), respectively.

2.1. Return Loss and VSWR

To investigate the performance of the proposed antenna configuration, the commercially available simulation software, CST MWS V9 based on finite integration technique was used for the required numerical analysis and optimization of geometrical parameters. To simulate the antenna, transient solver was chosen. During simulation, hexahedral mesh cell with 20 lines per lambda was selected. The geometrical parameters were adjusted carefully after performing a number of experimental iterations by using the option of parameter sweep in transient solver. Finally, the optimal parameters obtained for the proposed configuration are presented in Table 1.

Return loss is a convenient way to characterize the input and output signal sources. S_{11} represents how much power is reflected from the antenna. If $S_{11} = 0$ dB, it shows that all power is reflected from the antenna and nothing is radiated. Figure 3 shows the simulated return loss of proposed antenna with the optimized parameters which confirms dual-band operation at desired bands with reasonable bandwidth. As can be well-verified from this figure, the antenna shows a return loss of -20 and -32 dB at two strong resonating frequencies 3.48 and 5.25 GHz, respectively. A 50-ohm microstrip line is used to feed the patch for impedance matching. The simulated impedance bandwidths of the two distinct operating bands with 10-dB return loss are about 300 MHz (3.32–3.62 GHz) and 2.11 GHz (4.72–6.83 GHz).

Another parameter that is used to judge the performance of any antenna is its voltage standing wave ratio (VSWR) measurement. For an ideal match, the VSWR should be 1 which means no reflections. In our present design structure, it turns out to be 1.32 and 1.24 that is, VSWR < 2 and the impedance transformations ratio are 1:1.32 and 1:1.24 at 3.48 and 5.25 GHz, respectively. These values indicate that the antenna is very well-matched to a 50-ohm line allowing maximum power to be coupled through the line to antenna allowing for best results.

2.2. Effect of Dielectric Constant

The dielectric constant is varied from 4.3 to 4.7. The return losses with variation of Єr are depicted in Figure 4. As the Єr increases, the first and the second resonant frequencies are shifted to the left and return loss value decreases for the lower band. So the FR-4 substrate with dielectric constant 4.4 is preferred to cover the WLAN/multiple input multiple output (MIMO)/WiMAX/AMSAT/WAVE frequency bands.

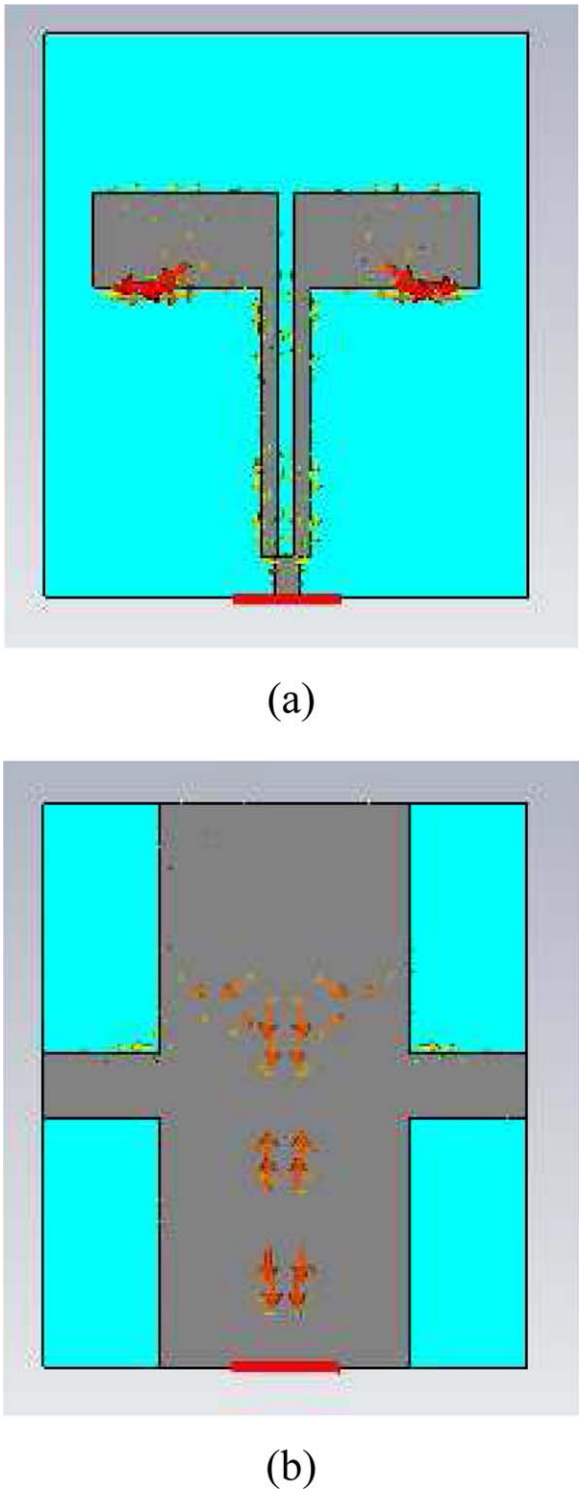

Figure 5 Surface current distribution of the proposed at (a) 3.48 and (b) 5.25 GHz. [Color figure can be viewed in the online issue, which is available at wileyonlinelibrary.com]

2.3. Current Distribution Results

To explain more details on the excited resonant modes of the proposed antenna, the simulated current distributions at two

Figure 6 Photograph of the proposed antenna. [Color figure can be viewed in the online issue, which is available at wileyonlinelibrary.com]

resonant frequencies of 3.48 and 5.25 GHz are shown in Figures 5(a) and 5(b). From these figures, it can be noticed that DGS was responsible for enhancing the impedance bandwidth for the upper band resonating at 5.25 GHz and inverted L-shaped patches fed by a microstrip line were responsible for resonance at 3.48 GHz. Further, a gap between a pair of L-shaped patches also play an important role in the sufficient excitation of two resonant modes covering WLAN/MIMO/WiMAX/AMSAT/WAVE wireless communication standards.

3. FABRICATION AND MEASUREMENT RESULTS

The simulated antenna after detailed parametric analysis and optimization was fabricated on a dielectric substrate named Epoxy Glass-FR4 ($\varepsilon_r = 4.4$, $\tan\delta = 0.0024$, $h = 1.6$ mm) and was studied experimentally. Available photolithography method with wet etching facility was adopted for fabrication of the prototype antenna and its photograph is shown in Figure 6. After fabrication, the return loss of the antenna was tested on Agilent E5071C vector network analyzer and the radiation performance was measured in the Anechoic Chamber at Millimeter Wave Laboratory, I.I.T-Roorkee, India. The measured return loss (blue curve) against frequency plot for this dual-band proposed antenna design covering multiple frequency bands is presented in Figure 7.

Measured return loss of proposed MSA indicates that the impedance bandwidths of the two distinct operating bands with 10-dB return loss were about 200 MHz (3.34–3.54 GHz) and 1.36 GHz (4.90–6.26 GHz) which are wide enough to cover the

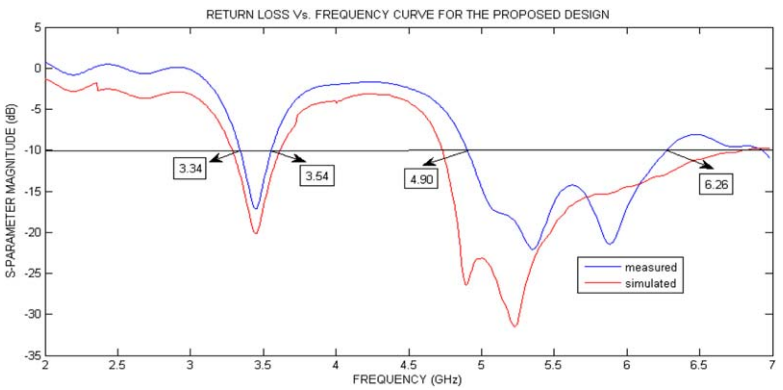

Figure 7 Comparison of simulated and measured return loss of the proposed antenna. [Color figure can be viewed in the online issue, which is available at wileyonlinelibrary.com]

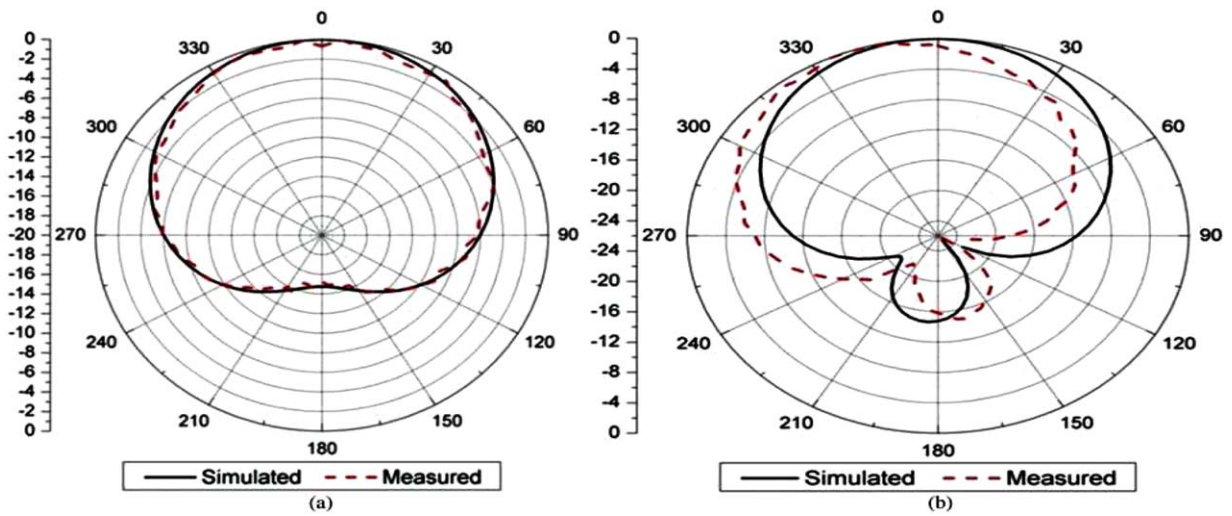

Figure 8 Simulated and measured (a) *E*-plane radiation pattern and (b) *H*-plane radiation pattern at 3.48 GHz. [Color figure can be viewed in the online issue, which is available at wileyonlinelibrary.com]

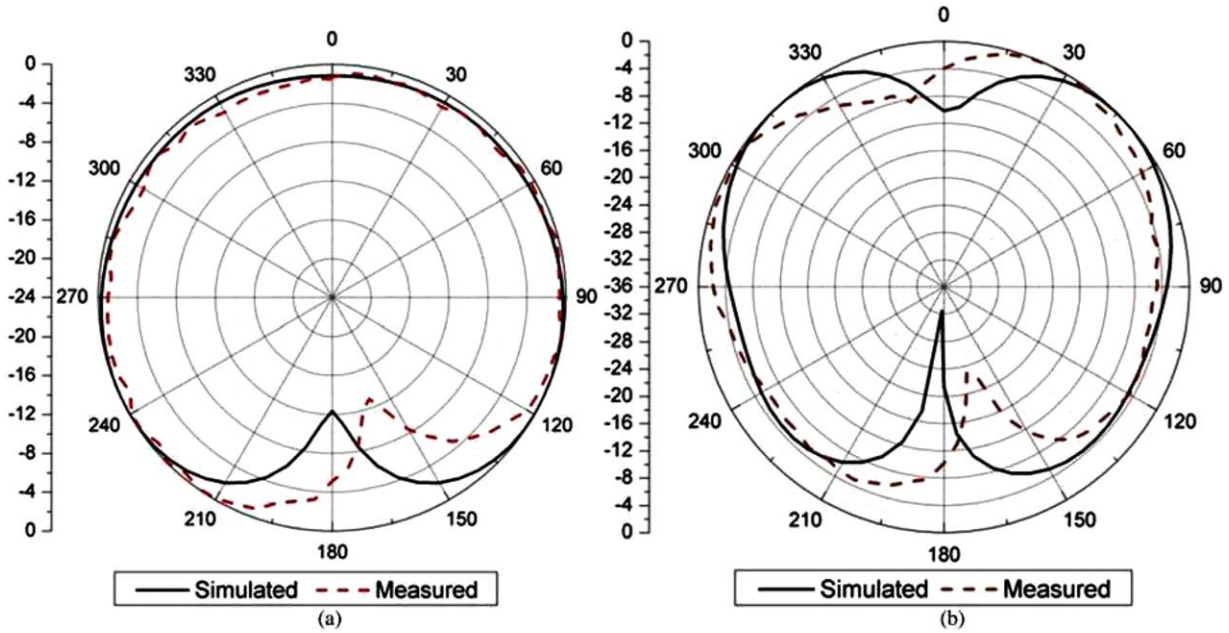

Figure 9 Simulated and measured (a) *E*-plane radiation pattern and (b) *H*-plane radiation pattern at 5.25 GHz. [Color figure can be viewed in the online issue, which is available at wileyonlinelibrary.com]

required bandwidths of 3.3–3.5, 5.15–5.35, and 5.725–5.825 GHz for WLAN, 3.3–3.5 GHz for MIMO, 5.25–5.85 GHz for WiMAX, 5.650–5.670 GHz for uplinks and 5.830–5.850 GHz for downlinks of AMSAT, and 5.9 GHz WAVE-IEEE 802.11p. The inverted L-shaped patches fed by a microstrip line were responsible for a resonance at 3.48 GHz, and DGS was responsible for enhancing the impedance bandwidth for the upper band resonating at 5.25 GHz. Further, a perfect gap between a pair of L-shaped patches also play an important role in the sufficient excitation of two resonant modes. The optimal values of parameters "d" and "L_{g1}" improved the impedance matching condition, gain, and radiation characteristics of the proposed antenna. Thus, using this specific antenna structure with DGS, a wide operating band with a bandwidth of 24% from 4.90 to 6.26 GHz can be achieved. A quite good agreement was seen between the simulated and measured results for the proposed antenna (Fig. 7). A little shift in both the resonating bands was observed during measurement which could be attributed to mismatching between the connector and the antenna feeder, fabrication errors, interference and noise.

Figures 8 and 9 depict both the simulated and measured far-field radiation patterns of the proposed antenna in the *E*-plane and *H*-plane at the operating frequency bands of 3.48 and 5.25 GHz, respectively. These results were normalized for setting the maxima 0 dB. Reasonable good agreement was found between the simulated and measured values of radiation patterns in two distinct operating frequency bands which validate the proposed design. Some slight differences between the simulated and measured field patterns may be attributed to alignment error and possible presence of interference and noise.

The simulated and measured gain curves are also shown for the two operating bands at 3.48 and 5.25 GHz in Figure 10. Gain measurements are done for the two frequency bands in the directions of their respective maxima using the substitution/gain

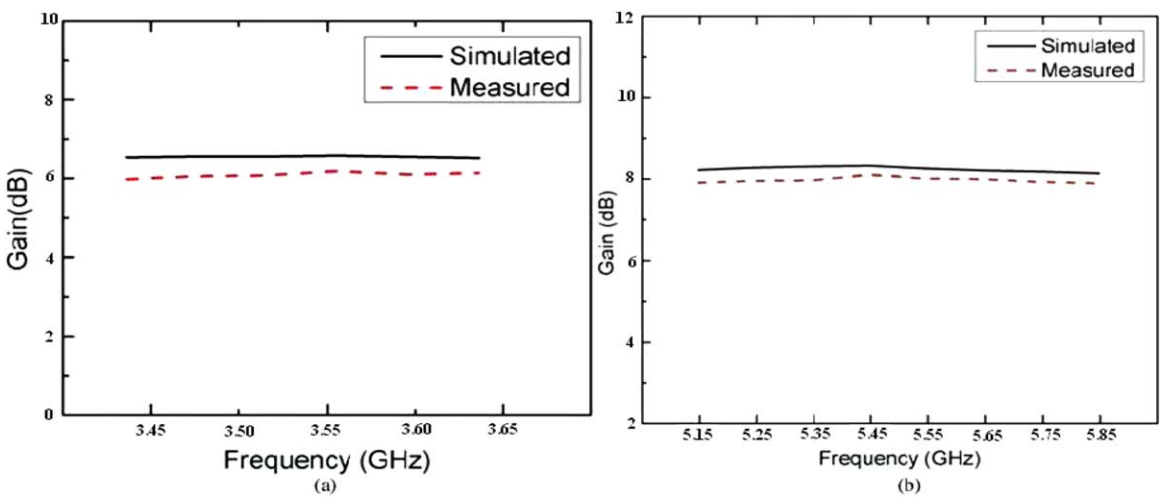

Figure 10 Simulated and measured gains of the proposed antenna at (a) 3.48 and (b) 5.25 GHz frequency bands. [Color figure can be viewed in the online issue, which is available at wileyonlinelibrary.com]

transfer technique with the help of a standard horn antenna with calibrated gain. Less than 0.6 dB of difference in the simulated and measured gains was observed which can be attributed to fabrication and measurement errors. As a result, the proposed antenna with stable and appreciable gain characteristics is very suitable to be integrated into the portable wireless terminals for WLAN/MIMO/WiMAX/AMSAT/WAVE application systems.

4. CONCLUSION

In this article, a compact, high-gain and dual-band MPA formed with a pair of inverted L-shaped patches and ┼-shaped ground plane is presented that is suitable for WLAN/MIMO/WiMAX/AMSAT/WAVE and other long-distance communication applications. The frequency bands with return loss below −10 dB cover 3.34–3.54 and 4.90–6.26 GHz with maximum gain values of 6.1 and 8.0 dB in the lower and higher frequency bands, respectively, thus making the proposed antenna appropriate for high-gain applications. The microstrip line feeding method enables direct feeding of the structure without using complicated impedance transformer or microstrip taper. The fabricated prototype on measurement shows reasonable impedance bandwidths of around 200 MHz (3.34–3.54 GHz) and 1.36 GHz (4.90–6.26 GHz) in two operating bands. Slight discrepancies between simulated and measured results are observed which may be mainly due to errors in fabrication process and possible presence of interference and noise. In this specific antenna structure, DGS has been incorporated which is actually responsible for the wide impedance bandwidth of 24% from 4.90 to 6.26 GHz. Taken as a whole, the performance of the antenna meets the desired requirements in terms of return loss, high gain, and VSWR at the two operating frequencies. From this article, it can be concluded that the performance of the microstrip antenna depends heavily on the dimensions of the inverted L-shaped patches and DGS been used. The type, thickness, and dielectric constant of substrate also contribute in the antenna performance. The proposed antenna production costs are reduced because of using a FR-4 substrate. It is seen that the proposed antenna having simple structure achieved very good performance and can be constructed with a lower cost. Hence, the proposed dual-band design will meet the requirements of various wireless communication standards with smaller size and can be easily integrated to microwave circuits for practical wireless applications.

ACKNOWLEDGMENTS

The authors are thankful to Dr. M.V. Kartikeyan, Millimeter Wave Laboratory, I.I.T, Roorkee, India, for providing necessary guidance and valuable comments while writing the research paper. Thanks are due to Mr. J. Malik for his help and cooperation.

REFERENCES

1. Y. Cao, C. Lu, and Y. Zhang, A compact dual band miniaturized antenna for WLAN operation, In: Proceedings of International Conference on Microwave and Millimeter Wave Technology, 2008, pp. 416–419.
2. Q. He, B. Wang, and J. He, Wideband and dual-band design of a printed dipole antenna, IEEE Antennas Wireless Propag Lett 7 (2008), 1–4.
3. M.J. Kim, C.S. Cho, and J. Kim, A dual band printed dipole antenna with spiral structure for WLAN application, IEEE Microwave Wireless Compon Lett 15 (2005), 910–912.
4. R.K. Joshi and A.R. Harish, A modified bow-tie antenna for dual band applications, IEEE Antennas Wireless Propag Lett 6 (2007), 468–471.
5. B.S. Izquierdo and J.C. Batchelor, A dual band belt antenna, In: Proceedings of International Workshop on Antenna Technology: Small Antennas and Novel Metamaterials, 2008, pp. 374–377.
6. C.I. Lin and K.L. Wong, Printed monopole slot antenna for internal multiband mobile phone antenna, IEEE Trans Antennas Propag 55 (2007), 3690–3697.
7. B. Kelothu, K.R. Subhashini, and G. Lalitha Manohar, A compact high-gain microstrip patch antenna for dual band WLAN applications, In: Students Conference on Engineering and Systems, SCES, 2012.
8. M. Wong, A.R. Sebak, and T.A. Denidni, Analysis of a dual-band dual slot omnidirectional stripline antenna, IEEE Antennas Wireless Propag Lett 6 (2007), 199–202.
9. K. Chung, S. Hong, and J. Choi, Ultrawide-band printed monopole antennas with band-notch filter, IET Microwave Antennas Propag 1 (2007), 518–522.
10. J. Kaur and R. Khanna, Design of coaxial fed microstrip patch antenna for Wi-MAX/IMT applications, Res J Eng Technol 4 (2013), 40–44.
11. K. Oh, B. Kim, and J. Choi, Design of dual and wideband aperture stacked patch antenna with double-sided notches, Electron Lett 40 (2004), 643–645.
12. K.G. Thomas and M. Sreenivasan, Compact triple-band antenna for WLAN/WiMAXapplications, Electron Lett 45 (2009), 811–813.
13. J. Kaur, M.V. Kartikeyan, and R. Khanna, Design of a multi-frequency wideband microstrip patch antenna for 5.2/5.5/5.8 GHz wireless applications, In: Proceedings of National Conference on Recent Trends in Microwave, July 30–August 1, 2012.
14. K. Lau, H. Wong, C. Mak, K. Luk, and K. Lee, A vertical patch antenna for dual-band operation, IEEE Antennas Wireless Propaga Lett 5 (2006), 95–97.
15. A.A. Eldek, Analysis and Design of Wideband Slot and Printed Antennas for Phased Array Antenna Systems, PhD Thesis (Electrical Engineering), University of Messisippi, Messisippi, November 2004.
16. R. Garg, P. Bhartia, I. Bahl, and A. Ittipiboon, Microstrip Antenna Design Handbook, Artech House, Norwood, MA, 1995.
17. A. Asrokin, M.K.A. Rahim, and M.Z.A.A. Aziz, Dual band microstrip antenna for wireless LAN application, In: Asia-Pacific Conference on Applied Electromagnetics, APACE, 2005.

COMPACT MICROSTRIP LOOP RESONATOR-BASED BANDSTOP FILTERS FOR SUB-GHz CHANNELS

Adam Rudziński[1,2]

[1] Institute of Radioelectronics, Warsaw University of Technology, Nowowiejska 15/19, 00-665 Warsaw, Poland; Corresponding author: adam.rudzinski@ire.pw.edu.pl

[2] SKA Polska Sp. z o.o., Al. Jerozolimskie 125/127 p. 406, 02-017, Warsaw, Poland

Received 2 August 2013

ABSTRACT: *This article presents two microwave bandstop filters based on microstrip loop resonators with capacitors. The filters have steep band edges, are compact and easy to fabricate. They are applicable for protection against strong signals in nearby channels. Construction of filters, capabilities of band shift compensation, and tuning are discussed.* © 2014 Wiley Periodicals, Inc. Microwave Opt Technol Lett 56:993–997, 2014; View this article online at wileyonlinelibrary.com. DOI 10.1002/mop.28202

Key words: *microstrip filter; microwave filter; loop resonators; channel protection; sub-GHz band*

1. INTRODUCTION

Filters are one of the important devices, necessary in most radio communication equipment. They are realized in many different